DOI: 10.31401/WS.2020.proc.14

Thermospheric Wind Variability at High Latitudes – the Wind Wall

Shepherd, M.G., Shepherd, G.G., Barreto, C.S., Cho, Y.M., Chen, Y.

Centre for Research in Earth and Space Science, York University, Canada
E-mail: mshepher@yorku.ca

Abstract

The report provides an overview of previously unrecognized neutral wind reversals in the daytime thermosphere at high latitudes, 50º – 70º, employing satellite observations by the WINDII experiment on the UARS satellite and the WACCM-X model simulations. The seasonal and local time variability with longitude and height is examined for a number of parameters characterizing the neutral thermosphere and ionosphere. A distinct and very persistent pattern of sharp zonal wind reversals from eastward to westward was observed at ~50ºE – 200Eº in the Southern hemisphere and 280ºE – 360ºE in the Northern hemisphere at altitudes from ~150 km to 300 km, independently of season. The observed westward wind speed reached -450 ms^{-1}.

Introduction

There have been extensive studies of the neutral thermospheric dynamics at high latitudes but more remains to be explored, in part because of the lack of observations. *Richmond et al.* (2003) investigated high-latitude winds observed by the Wind Imaging Interferometer (WINDII) on board the Upper Atmosphere Research Satellite (UARS) [*Shepherd et al*., 2012] and found winds exceeding 300 ms^{-1} with well-defined correlation with the interplanetary magnetic field B_y and B_z components. *Thayer et al.* (1995) investigated ion and neutral winds observed at Thule, Greenland at 77.5ºN geographic latitude and found that during disturbed conditions the sunward ion winds reached velocities of 1000 ms^{-1}, while the neutral winds marked velocities of the order of 500 ms^{-1}. *Dhadly et al.* (2017) combined wind data from many sources to generate neutral wind maps for quiet geomagnetic conditions. A second study by *Dhadly et al.* (2018) provided such maps for disturbed conditions. Those presentations were polar projections of magnetic latitude as a function of magnetic local time, but did not contain any longitude information.

Recently a series of studies were conducted employing daytime WINDII observations of oxygen airglow emission rates, Doppler temperature and neutral (zonal and meridional) winds and the Whole Atmosphere Community Climate Model including the thermosphere and ionosphere extension (WACCM-X) simulation [*Shepherd and Shepherd*, 2018; M. *Shepherd et al.*, 2019; *Liu et al.*, 2019] which revealed localized zonal wind reversals from eastward to westward that occurred frequently in the high-latitude thermosphere with strong westward winds reaching velocities of -450ms^{-1} and greater, always at the same longitudes of 50ºE – 200ºE in the Southern hemisphere and 280ºE – 360ºE in the Northern hemisphere at the same latitude of ~ 60º – 70º in both hemispheres. The zonal wind observations derived from Doppler shifts of the $O(^1S)$ green line of atomic oxygen at 557.7 nm reversed direction from eastward (positive) to westward (negative) so abruptly that *Shepherd and Shepherd* (2018) suggested the name "wind wall" for this sharp reversal. M. *Shepherd et al.* (2019) extended the study of those first unique observations by making use of the $O(^1D)$ red line of atomic oxygen at 630 nm, which occurs at higher altitudes (150 – 310 km for the WINDII observations) and from which Doppler temperatures can also be obtained. The thermospheric $O(^1D)$ 630 nm airglow emission was chosen because of the information it could provide on the electron density and neutral winds in the F-region of the ionosphere. Data for two Southern Hemisphere seasons, summer solstice and fall equinox were examined.

The present report is intended to present some highlights from these studies to describe the wind wall and together with some new WACCM-X model results to illustrate its dynamics.

More detailed information on the wind wall morphology can be found in the above mentioned references.

In describing the results that follow and in particular those pertinent to the neutral winds the terms 'peak/maximum' are used to describe the maximum eastward/northward (positive) directions of the zonal/meridional winds. Accordingly, a 'trough/minimum' refers to westward/southward (negative) directions of the zonal/meridional winds.

Results

a) WINDII thermospheric observations

The nature of the wind wall in illustrated in Fig. 1 where the observed WINDII zonal winds obtained from the $O(^1S)$ emission are shown as a function of longitude and height over a period of several consecutive days. The left panel (A) shows the zonal wind during DoY (day of year) 73 – 79 (March 13 – 19), 1996 at 60ºS – 70ºS, while the right panel (B) shows the same for DoY 275 – 280 (October 2 – 7), 1995 at 60ºN – 70ºN.

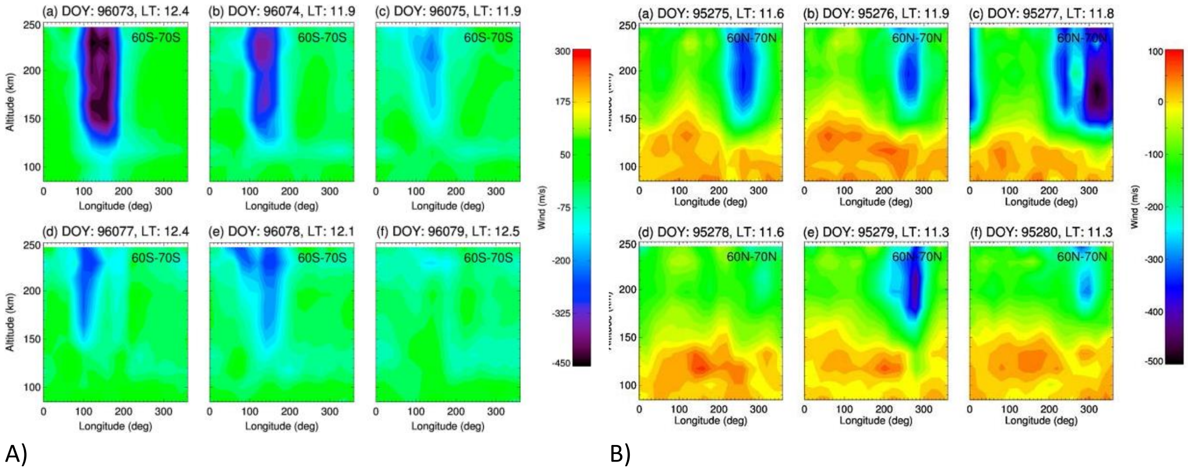

Fig. 1: WINDII zonal wind from the $O(^1S)$ emission as a function of longitude and altitude for: (A) DoY 73 – 79 (March 13 – 19), 1996 (left panel) at 60ºS – 70ºS, and (B) DoY 275 – 280 (Oct 2 -7), 1995 at 60ºN – 70ºN.

Here and elsewhere the convention is that eastward zonal wind is positive, while westward zonal wind is negative. As can be seen the reversal of the zonal wind from predominantly eastward to westward persistently occurs around 50ºE – 200ºE in the Southern hemisphere and at around 280ºE – 360ºE in the Northern hemisphere. Although it varies in magnitude and altitude extension from day to day, its boundaries are sharp and extend from ~ 150 km to at least 250 km height, based on the $O(^1S)$ emission and wind observations. The local times of these zonal wind reversals for this period are around noon, 12 LT.

Fig. 2 shows the WINDII meridional wind for the period of DoY 96073 – 96079 and latitude band of 60ºS – 70ºS. Following the convention, here the positive values correspond to northward direction, while the negative values are for southward direction. Similar to the zonal wind, the meridional wind also shows sharp reversal of direction over the same longitude range of ~ 50ºE to 200ºE. Its longitudinal extension is broader than that of the zonal wind and appears accompanied by a northward wind peak east of the southward (negative) peak. The meridional wind is weaker than the zonal wind, ranging within ± 200 ms^{-1}, compared to -450 ms^{-1} to 300 ms^{-1}. Examining a series of zonal wind vertical profiles along a WINDII orbit traversing the 100ºE - 200ºE region at 60ºS – 70ºS on DoY 96073 for example (not shown here), showed that while profiles on the edge of the zonal wind reversals were almost vertical with wind velocity of ~ 0 ms^{-1}, within the reversal zone individual wind profiles indicated westward wind speeds of up to -650 ms^{-1}, with most of the observations of -450 ms^{-1}.

WINDII observations of the upper thermosphere daytime fields of $O(^1D)$ volume emission rate (VER), neutral zonal and meridional winds and Doppler temperature from 170 km to 310 km were also available providing an opportunity to examine the morphology of the wind wall to higher altitude. Fig. 3 shows some of these observations as a function of longitude and altitude in the Southern hemisphere at 50ºS – 70ºS. The two days shown are representative of a series of consecutive days of observations during March/April 1994 (fall equinox), (left column) and January 1995 (summer solstice), (right column) corresponding to local time of 8 – 13LT and 12 – 16 LT, respectively.

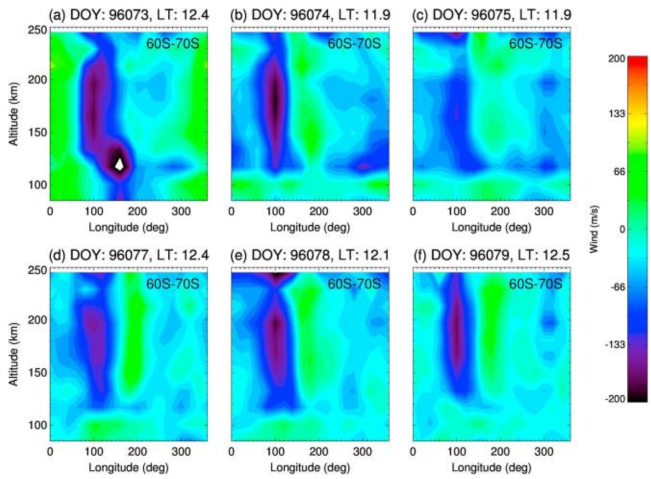

Fig. 2: Meridional wind for the same period as in Fig. 1. Note that for day 79 in panel 2f there is a strong wind wall signature although it does not exist for the zonal wind in Fig. 1f.

What is remarkable in these plots is the fact that all fields considered reach peak at the same longitude range of about 50ºE to 200ºE independently of season (fall equinox or summer solstice) or local time (morning vs afternoon). At the time of the peak $O(^1D)$ VER used as a proxy for electron density, around 220 – 240 km height the zonal wind reversed direction from prevailing eastward to westward. During fall equinox the westward zonal wind reached velocity of -330 ms^{-1}. The meridional wind also showed an abatement or reversal of direction to southward around 100ºE, accompanied with an increase/reversal to poleward around 200ºE. This pattern is very similar to the $O(^1S)$ meridional wind observations in Fig.2. Finally, the $O(^1D)$ temperature showed a peak/trough pattern with a broad peak centred around 100ºE, increasing in magnitude with height and a trough between 200ºE and 300ºE, here more pronounced in the DoY 95004 observations.

b) WACCM-X simulations of the wind wall

WACCM-X [*Liu et al.*, 2018, and references therein] is a comprehensive numerical model, which produces neutral atmosphere 3-D temperature, density, winds, composition, ionospheric parameters and electric potential fields. It is a part of the NCAR Community Earth System Model and extends the description of the neutral atmosphere up to 500 – 700 km altitude. The thermospheric and ionospheric components of WACCM-X add neutral species composition, electron and ion density, as well as ion and electron temperatures. The most notable additions are the fully coupled low and middle latitude electrodynamics, dynamical transport of O^+ and high latitude forcing by the magnetospheric electric fields and specific heat [*Liu et al.*, 2018]. The effects of geomagnetic activity are incorporated in WACCM-X by applying the Heelis empirical convection pattern, based on the geomagnetic Kp index. Fig. 4 shows maps of

WACCM-X simulations of electron density, neutral temperature, zonal and meridional winds at 200 km height for the latitude band of 50ºN – 80ºN, on DoY 95278 (October 5, 1995). The results are for the "specified dynamics" version of the model constrained by the meteorology from the Modern-era Retrospective Analysis for Research and Application 2 (MERRA2) [*Liu et al.*, 2018 and references therein]. For the simulations presented here the model was run on the Niagara supercomputer SciNet (hhtp://www.scinethpc.ca/niagara/).

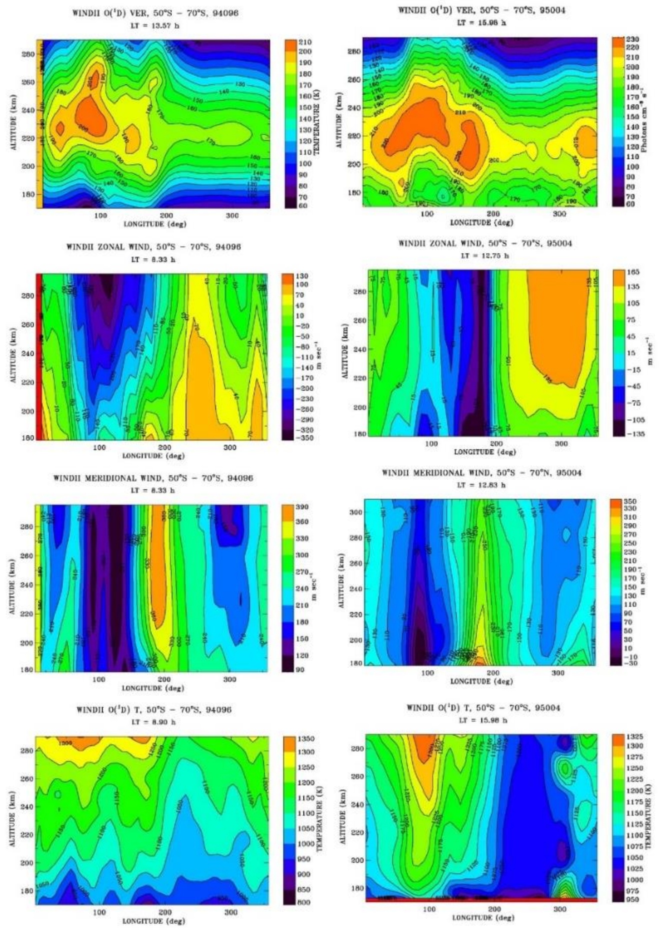

Fig. 3: WINDII O(^{1}D) VERs, neutral winds and Doppler temperature at 50ºS – 70ºS as a function of longitude and altitude for April 6, 1994 (DoY 94096) (left column) and January 4, 1995 (DoY 95004) (right column).

From Fig. 4 it is easy to see that the westward zonal wind follows closely the crest of the electron density along the auroral oval with the geomagnetic pole in 1995 at 79.4ºN and 288.6ºE, and appears to be on the poleward side of the electron density crest, which in turn outlines the auroral oval. DoY 95277 (October 4, 1995) shown here is the same, shown in Fig 1c, right panel (B), with Ap of 51. The reader is reminded that while the plots in Figs. 1&2 are composites of all observations within the ± 60º – 70º latitude band, as a function of longitude and height, Fig. 4 shows the mapping of the respective parameters in longitude and latitude at a selected height, e.g. 200 km. The westward wind reached velocity of -550 ms^{-1} at its peak around 350ºE – 50ºE and ~300 – 350ms^{-1} at ~ 250ºE – 330ºE, in agreement with the WINDII observations. There is about a 200 K temperature variation throughout the latitude band considered, with a cold temperature anomaly around 100ºE extending poleward to ~ 67ºN that is similar to the anomaly seen in Fig. 3 (the bottom row). The meridional wind peaks around 150ºE – 300ºE poleward of the auroral oval.

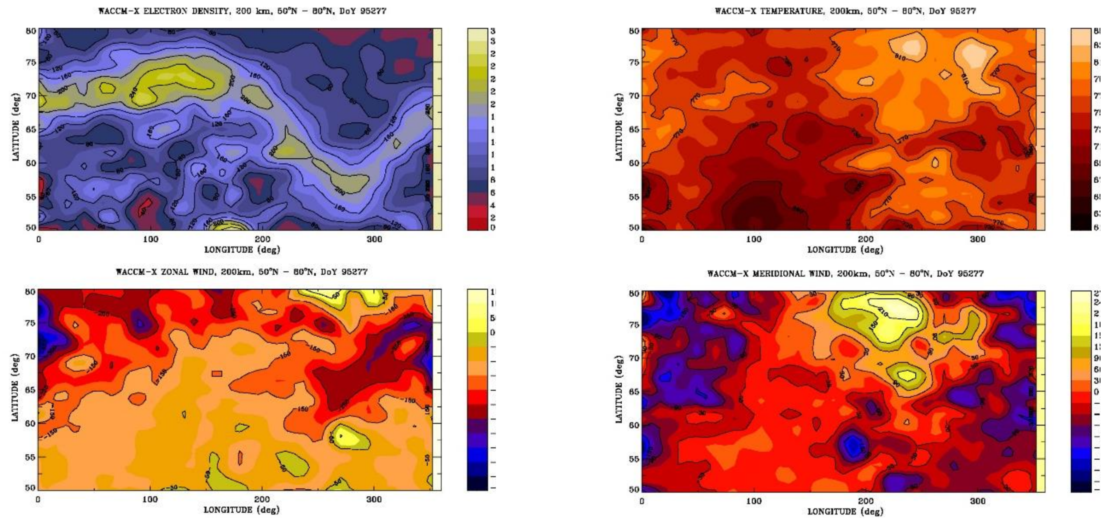

Fig. 4: WACCM-X model simulations of electron density, temperature and neutral (zonal and meridional) winds at 50ºN – 80ºN as a function of longitude at 200 km height for October 4, 1995 (DoY 95277).

Discussion

One of the first reports on the longitudinal variability of the neutral atmosphere at Southern middle and high latitudes was by *Laux and von Zahn* (1979) employing monopole mass spectrometer data from the Esro 4 satellite. They reported drastic changes in the [O]/[N_2] ratio observed between 50ºS – 80ºS and 110ºE to 180ºE geographic, within the vicinity of the geomagnetic pole, but shifted by ~ 10º in latitude toward the equator. As is presented in the current report the N_2 and O extreme variations occurred at the same longitude range independently of local time, remaining fixed to a limited longitude band. The persistence of the observed phenomenon and the lack of strong correlation with geomagnetic activity led *Laux and von Zahn* (1979) to the conclusion that this is a regular feature associated with thermospheric air motion.

Various studies on the seasonal and longitudinal variability of ionospheric daytime electron density have shown that it exhibits variability, related to changes in the thermo-spheric composition, in particular of the [O]/[N_2] ratio. *Millward et al* (1996) proposed a theory to explain the observed seasonal and semi-annual variations of electron density only through the longitudinal dependence of the interface between the solar-driven low/midlatitude neutral atmosphere circulation and the geomagnetically driven high latitude circulation, where the latitude of the interface depends on longitude. In the vicinity of the magnetic pole the magnetically driven circulation extends to relatively low geographic latitudes, and on the dayside its interaction with the neutral atmosphere circulation occurs at a geographic latitude of about ~ 50º – 65º. As was shown there is a longitudinal "wind wall" at about ± 63º – 66º in both hemispheres where the neutral wind velocity decreases and/or reverses direction affecting the variability of the oxygen airglow ($O(^1S)$, $O(^1D)$), temperature and [O] observed. An interesting feature in the observed variability was the fact that the peaks of all parameters considered (the $O(^1S)$ and $O(^1D)$ VER, temperature, zonal and meridional winds) in the vicinity of the magnetic pole were a persistent longitudinal feature independent of season and daytime local time. This is even more striking considering the fact that the observations are for different although consecutive days and different local times determined by the precession of the WINDII/UARS orbit. Given the fact that the geomagnetic pols in 1995 were at 79ºS and 109ºE in the Southern hemisphere and 79ºN, 289ºE, in the Northern hemisphere, they are very closely positioned to the regions where the reversal of the zonal wind and the wind wall are observed. The connection of the thermospheric wind reversals to the geomagnetic field and further coupling to the magnetosphere requires further investigation at latitudes higher than are available from WINDII, and so this will be a subject of future studies.

Conclusions

1. Between longitudes of 50ºE – 200ºE in the Southern hemisphere and 280ºE – 360ºE in the Northern hemisphere and at 60º – 70º latitudes there is a wind wall of extreme velocity reversals to westward zonal and southward meridional winds regularly -450 ms^{-1} and -200 ms^{-1}, respectively. Zonal winds could reach velocities of up to -650 ms^{-1}, observed when WINDII's most poleward orbit (at 72º geographic, 82º geomagnetic), cuts through the polar cap extreme wind field. It was suggested that the wall is the boundary between the strong westward polar cap winds and the weaker eastward winds equatorward of that.
2. Comparisons between the WINDII observations and WACCM-X simulations are in generally good agreement in describing the wind wall. The model simulations have shown that the appearance of the wind wall is modulated by the solar and geomagnetic activity. For high solar and geomagnetic active periods the wind wall is very pronounced and the westward zonal winds within the wall region are very strong.

References

Dhadly, M. S., Emmert, J. T., Drob, P. D., et al. (2017). Seasonal dependence of northern high latitude upper thermospheric winds: A quiet time climatological study based on ground-based and space-based measurements. J. Geophys. Res.: Space Phys., 122, 2619–2644. https://doi.org/10.1002/2016JA023688

Dhadly, M. S., Emmert, J. T., Drob, P. D., et al. (2018). Seasonal dependence of geomagnetic active-time northern high-latitude upper thermospheric winds. J. Geophys. Res.: Space Phys., 123(1), 739–754. https://doi.org/10.1002/2017JA024715

Laux, U., & von Zahn, U. (1979). Longitudinal Variations in Thermospheric Composition Under Geomagnetically Quiet Conditions. J. Geophys. Res., 84 (A5), 1942 – 1946.

Liu, H.-L., Bardeen, C. G., Foster, B. T., et al. (2018). Development and validation of the whole atmosphere community climate model with thermosphere and ionosphere extension (WACCM-X 2.0). J. Adv. Model. Earth System, 10, 381– 402. https://doi.org/10.1002/2017MS001232

Liu, S., Shepherd, G. G., Chen, Y., Shepherd, M. G., & Bhutia, S. (2019). WINDII observations and WACCM-X simulations of high-latitude winds under different solar radio flux and geomagnetic disturbance conditions. J. Geophys. Res.: Space Physics, 124, 6087–6096. https://doi.org/10.1029/2019JA026864

Millward, G. H., Moffett, R.J., Quegan, S., & Fuller-Rowell, T.J. (1996). Ionospheric F2 layer seasonal and semiannual variations. J. Geophys. Res., 101, 5149 – 5156, https://doi.org/10.1029/95JA03343 .

Richmond, A. D., Lathuillère, C., & Vennerstroem, S. (2003). Winds in the high-latitude lower thermosphere: Dependence on the interplanetary magnetic field. J. Geophys. Res., 108(A2), 1066. https://doi.org/10.1029/2002JA009493

Shepherd, G.G., Thuillier, G., Cho, Y.-M., et al. (2012). The wind imaging interferometer (WINDII) on the upper atmosphere research satellite: A 20 year perspective. Rev. Geophys., 50, RG2007 https://doi.org/10.1029/2012RG000390.

Shepherd, G. G., & Shepherd, M. G. (2018). High-latitude observations of a localized wind wall and its coupling to the lower thermosphere. Geophys. Res. Lett., 45, 4586–4593. https://doi.org/10.1029/2018GL077722

Shepherd, M., Shepherd, G., & Codrescu, M. (2019). Perturbations of $O(^1D)$ VER, temperature, winds, atomic oxygen, and TEC at high southern latitudes. J. Geophys. Res.: Space Phys., 124. https://doi.org/10.1029/2019JA026480

Thayer, J. P., Crowley, G., Niciejewski, R. J., et al. (1995). Ground-based observations of ion/neutral coupling at Thule and Qânâq, Greenland. J. Geophys. Res., 100, 12,189 – 12,199. https://doi.org/10.1029/95JA00131